Maxillary Changes Following Facial Bipartition – A Three-Dimensional Quantification

Alexander J **Rickart**, MFDS[1], Lara S **van de Lande**, MD[2], Eimear **O'Sullivan,** MRes[3], Juling **Ong**, FRCS[2], Daljit S **Gill**, FDS RCS[1], Robert D **Evans**, FDS RCS[1], Silvia **Schievano,** MEng PhD[2], David J **Dunaway**, FRCS[2]

1. Department of Oral and Maxillofacial Surgery & Craniofacial Unit, Great Ormond Street Hospital for Children, London, UK.
2. UCL Great Ormond Street Institute of Child Health, London, UK & Craniofacial Unit, Great Ormond Street Hospital for Children, London, UK.
3. Department of Computing, Imperial College London, London, UK.

Corresponding author:

David J. Dunaway, Professor of Craniofacial Surgery

Craniofacial Unit, Great Ormond Street Hospital for Children

Great Ormond Street

London. WC1N 3JH

Email: David.Dunaway@gosh.nhs.uk

Conflicts of Interest

The authors have no conflicts of interest to declare nor do they have a financial interest in any of the products, devices, or drugs mentioned in this manuscript.

Funding

This work has been funded by Great Ormond Street Hospital for Children Charity (Grant No. 12SG15), the Engineering and Physical Sciences Research Council (EP/N02124X/1) and the

European Research Council (ERC-2017-StG-757923). This report incorporates independent research from the National Institute for Health Research Biomedical Research Centre Funding Scheme. The views expressed in this publication are those of the authors and not necessarily those of the NHS, the National Institute for Health Research or the Department of Health. The funders had no role in study design, collection, analysis and interpretation of the data, decision to publish, or preparation of the manuscript.

SUMMARY

Introduction

Children with Apert syndrome have hypertelorism and midfacial hypoplasia, which can be treated with facial bipartition (FB), often aided by rigid external distraction (RED). The technique involves a midline osteotomy that lateralises the maxillary segments, resulting in posterior cross-bites and midline diastema. Varying degrees of spontaneous realignment of the dental arches occurs postoperatively. This study aims to quantify these movements and assess whether they occur as part of a wider skeletal relapse or as dental compensation.

Methods

Patients who underwent FB and had high quality CT-scans at the pre-operative stage, immediately post-surgery, and later postoperatively were reviewed. DICOM files were converted to three-dimensional bone meshes and anatomical point-to-point displacements were quantified using non-rigid iterative closest point registration. Displacements were visualised using arrow maps, thereby providing an overview of the movements of the facial skeleton and dentition.

Results

Five patients with Apert syndrome were included. In all cases, the arrow maps demonstrated initial significant anterior movement of the frontofacial segment coupled with medial rotation of the orbits and transverse divergence of the maxillary arches. The bony position following initial surgery was shown to be largely stable, with primary dentoalveolar relapse correcting the dental alignment.

Conclusion

This study showed that spontaneous dental compensation occurs following FB without compromising the surgical result. It may be appropriate to delay active orthodontic for six-months post-operatively until completion of this early compensatory phase.

KEYWORDS

Apert; Hypertelorism; Dentition; Orthodontics; Craniofacial Surgery

INTRODUCTION

Apert syndrome typically involves complex craniosynostosis, midfacial hypoplasia, orbital hypertelorism and syndactyly. As a result, functional difficulties ranging from elevated intracranial pressure and compromised vision through to sleep apnoea and limited dexterity may be encountered[1,2].

To address the midface concavity and hypertelorism seen in Apert syndrome, facial bipartition (FB) with or without rigid external distraction (RED) is often the surgical technique of choice. This procedure is the product of a number of historical developments in craniofacial surgery. Ortiz-Monasterio *et al.* built on previous descriptions by Firmin *et al.* and Tessier to develop the monobloc advancement, which has proven to be effective in the correction of midfacial hypoplasia and for increasing the orbital volume across the FGFR2 family of craniofacial dysostoses, such as Crouzon and Pfeiffer syndrome[3-5]. However, this approach failed to reduce the inter-orbital width. The median faciotomy, described by van der Meulen in 1979 and refined by Tessier to become the facial bipartition, addressed this issue and provided the ability to rotate the orbits medially[6,7]. Originally used in the correction of hypertelorism, it also lent itself well to the management of the complex Apert phenotype. Following these developments, a further paradigm shift in cranio-maxillofacial surgery took the form of distraction osteogenesis, a technique that allowed more stable movements without the need for extensive grafting[8-10]. Thus, FB with RED is the culmination of these three techniques. It has the functional capacity to potentially relieve sleep apnoea and provide corneal protection, with the aesthetic component focussing on reducing the inter-orbital width and addressing the midfacial biconcavity[11]. As a by-product of the midline osteotomy, a variation of surgically assisted rapid palatal expansion (SARPE) takes place, resulting in a midline diastema and significant cross bite around the midfacial pivot of the bipartition[12,13].

In addition, FB with RED has the potential to provide a vertical discrepancy between the maxillary segments if a particularly asymmetric orbital movement is required.

Owing to concerns that orthodontic pressures to realign the arches early may exert undue pressures on the consolidating bone and stimulate relapse of the orbital position, active orthodontic treatment is not undertaken for the first three to six months following surgery. Furthermore, lack of bone in the midline could be insufficient to support the incisal roots when readdressing the resultant diastema. However, a prior series of twenty cases showed that only two required alveolar bone grafting at a later date[11].

Using a computerised three-dimensional quantification methodology, this study aimed to analyse the movements of the dental arches, dentition and orbits following FB. It would be reasonable to assume that substantial occlusal derangement would be challenging to correct later orthodontically; however, it has been noted that the dental arches collapse inwards following completion of the distraction. This study aims to objectively assess in a 3-dimensional fashion whether the spontaneous realignment is predominantly a dental compensation, part of a global relapse of the bipartitioned frontofacial segments, or a combination of the two.

MATERIALS AND METHODS

Dataset

Ethical approval was gained from the Joint Research and Development Office at the Great Ormond Street Hospital for Children, London, UK (GOSH) before retrospective review of the craniofacial database was undertaken. All patients who underwent FB with or without

RED between 2004 and 2019 were identified and were included if high-resolution Computerized Tomography (CT)-scans were available for 3D reconstruction at the pre-operative stage, immediately post-surgery or completion of distraction, and in the later post-operative phase. CT-scans with 1-millimetre slice thickness were required. The late post-operative phase was considered as more than 120 days following surgery. Additional demographic information was collected from the patient files alongside perioperative orthodontic records.

Data processing

Data processing was performed using the following semi-automated pipeline. All CT images were converted to three-dimensional (3D) bone meshes using Mimics InPrint 3.0 (Materialise NV, Leuven, Belgium). These meshes were then cleaned using thresholding and isolation techniques to leave the cranium and midfacial bony structures, with the mandible excluded. Meshes were imported into 3Matic Software (Materialise NV, Leuven, Belgium) for Rigid Iterative Closest Point Registration (RICP). This process rigidly aligns the pre- and postoperative meshes using landmark points chosen to ensure that only the effects of the FB were taken into consideration when calculating bone and dental movements. For the RICP, ten landmarks were used on the posterior cranial base: basion and opisthion of the foramen magnum, the most anterior point of the carotid canal bilaterally, the mid-point of the spheno-occipital synchondrosis, and five patient specific landmarks on the posterior cranial vault. All postoperative 3D meshes were aligned to the preoperative 3D mesh for consistency. Each mesh was given their own colour in the 3Matic Software. Good alignment was demonstrated by a marbling effect of these colours. (*Figure 1*).

Quantification

To objectively quantify movements of the frontofacial segments following surgery, the initial pre-operative mesh was compared with the immediate postoperative 3D mesh (i.e. in case of FB alone, directly following surgery, and, in case of FB with RED, after completion of distraction). To assess the displacements in the post-operative period, the meshes were compared sequentially with those chronologically preceding them. Thus, the immediate post-operative scan was compared with the pre-operative CT-scan, while the late post-operative CT-scan was compared with the immediate post-operative CT-scan. In case where multiple late post-operative CT-scans were available, the latest was compared with the CT-scan immediately prior to it.

Quantification was undertaken using non-rigid ICP (NICP) following the process described in detail by Booth *et al.*[14]. NICP utilises manually placed landmarks within the mesh to guide the registration. Twenty-three anatomical points, as demonstrated in *Figure 2*, were used (R3DS WRAP v3.4, Voronezh, Russia). The meshes were landmarked twice by A.J.R. and E.O.S. with a week interval between observations to minimise memory bias. The mean point between the two landmarks (from the two-time landmark process) was used to calculate absolute point-to-point distances and achieve dense anatomical correspondence. The frontofacial movements could then be measured using in-house software. Further analysis was undertaken by isolating x-axis, transverse movements between paired landmarks to assess maxillary and inter-orbital width.

Arrow maps were used to visualise the results of the anatomical point-to-point movements providing an overview of the global displacements across the entire facial skeleton and dentition.

RESULTS

Thirty patients underwent FB during the study period, of which five patients with Apert syndrome met the strict inclusion criteria for quantification; four of these were FB with RED, with one undergoing FB without distraction. Due to the heterogeneity and small numbers of the study population, each case was considered individually (*Supplemental Table 1*).

All landmarks that were used for both RICP and non-rigid ICP were shown to be consistent within one standard deviation across the two separate time points. The mean intra-observer error was less than one millimetre for 15 of the 23 landmarks. The maximum intra-observer error was 1.61 mm (*Supplemental Table 2)*.

Absolute anatomical point-to-point distances are summarised in *Supplemental Table 3*. However, the results are best represented via the arrow maps in *Figure 3* alongside *Video 1* as they highlight the vectors of movement at each vertex of the meshes.

All patients, despite being heterogeneous in terms of age and phenotypic expression, show a consistent pattern. The images illustrating the initial post-operative results show a significant anterior and a minor inferior movement of the frontofacial segment with medial rotation of the orbits and divergence of the maxilla from the midline. The displacements in the later post-operative period demonstrate the relatively stable bony position, with a minimal superolateral counter-rotation of the orbits and consistent maxillary position. In contrast, movements at the dento-alveolar level demonstrate a primary dental compensation that corrects the surgically induced malocclusion. It is worth noting that patients B and D underwent pre-surgical orthodontics to open a midline diastema to facilitate the sagittal osteotomy. Only patient D underwent post-operative orthodontics during the study period, and these displacements can be seen in the dento-alveolar region in the arrow map comparing the second and third post-operative meshes in *Figure 3*.

The postoperative skeletal stability was further confirmed by a consistent inter-orbital width and a stable distance between the greater palatine foramina. A median relapse of 1.8mm (range, 0.0 to 4.1mm) was seen between the supra-orbital foramina and 0.7mm between the greater palatine foramina (range, 0.1 to 3.7mm). In both instances, the upper limit of the range comes from patient D, with the other patients showing lesser degrees of movement. In contrast, the maxillary width measured at the dental level of the mesio-buccal cusps of the first molars narrows markedly following the initial post-operative period. This is especially notable in patients C, D and E where the arch narrows between 3.2 and 3.6mm (*Supplemental Table 4*.).

DISCUSSION

Using a three-dimensional semi-automated methodology, this study demonstrates that the relapse of the dental arches following FB is predominantly the result of dental compensation.

The movements achieved through FB with RED are in-keeping with those previously described and remain invaluable in the management of Apert syndrome[15,16]. Focussing on the maxillary movements, there is a greater divergence in the anterior maxilla compared to the buccal segments. This is likely accentuated by the preferential mid-facial distraction elicited by the RED-frame, whereby the lateral aspects are advanced to a lesser degree[11,17]. Where FB was undertaken without distraction, the primary indication for surgery was to address midfacial form and although the pattern of movement was similar to the other cases, the advancement was much smaller.

The position of the frontofacial bony segments remains largely stable post-operatively which is consistent with previously reported outcomes suggesting an absence of relapse and cessation of growth following surgery[18,19]. Stability remains homogenous amongst different age groups but the hindering of further growth following surgery means that younger patients have a tendency towards functional relapse.

As such, impairment of the upper airway, raised intra-cranial pressure or the need for ocular protection are the main indications for early intervention, with the aesthetic component only considered later down the line. The timing of such significant surgery is a contentious issue and should be taken on a case-by-case basis. However, it may be best delayed until early adolescence unless being utilised to avert crisis, as was the case for patient C. Undertaking surgery before the child progresses to secondary school likely provides the best balance between allowing for growth and providing psychological benefit during formative years.

In spite of the stable bony position, dental compensation is stimulated by the expansion of the maxillary arch form and resultant increase in buccal soft-tissue pressures[20]. Thus, it is expected that, by the time active orthodontic treatment is started, occlusal complications of bilateral scissor-bites or significant cross-bites is seldom seen. Studies have shown that surprisingly few patients require bone grafting in the midline to support the roots of the central incisors; this can be attributed to the stimulation of osteoblastic activity throughout the distraction process[11].

As previously described, three-hole threaded fixation plates are placed at the nasion, with one on each side of the supraorbital bar and one on either side of the pyriform fossa. A central screw placed in the plates is then passed through the skin and wires attached to gain traction from the RED frame[11]. For patient D, a small miniplate was also placed just below the anterior nasal spine in the midline of the maxilla. Although not undertaken in any of the above cases, loop wire fixation is an alternative in the pyriform region, and this can help avoid damage to the roots of the teeth[21]. It is hard to say how the type of fixation used, especially at the maxillary level, may influence the changes to the occlusal relationship during distraction, but following consolidation is unlikely to play a significant role.

On the later stage CT-scans, some minimal lateral and posterior movements of the orbits following surgery, were demonstrated. This pattern is the direct antithesis of the surgical aim, representing minor relapse. Interestingly, this is seen most markedly at the superior orbital rim and not as part of a larger displacement of the distracted region.

One patient does not fit the above pattern so clearly. After an initial correction of 12.3 mm of the supra-orbital foramina, patient D demonstrated a 9.6 mm relapse in the x-axis. However, this is not reflected in all the peri-orbital landmarks, which otherwise remain stable both in the x-axis measurements and on the arrow maps. Similarly, the transverse distance between the greater palatine foramina initially widens by 8 mm but then converges by 3.7 mm over the following year. This patient had particularly pronounced midfacial hypoplasia and hypertelorism and the larger movements used to overcome this may be more prone to relapse. Additionally, this pattern may also have be influenced by difficulties in landmarking the supra-orbital region post-operatively and the time elapsed between pre-operative CT-scans and the operation itself. Interestingly, this was also the only patient to undergo active postoperative orthodontics during the study period.

Limitations

This study considers a small cohort relative to the volume of surgery being carried out at *Great Ormond Street Hospital for Children.* This was largely due to the use of Spiral Assisted Computed Tomography for post-operative imaging which enables quick acquisition and three-dimensional reconstruction but lacks sufficient detail for three-dimensional morphometrics. With a clinical change of scanning protocol going forwards, more data will be available, with potential consideration to incorporating intra-oral scanning into the workflow to improve accuracy.

The study group has a wide age range (6-21 years of age) which is representative of the larger cohort treated at our unit. However, there is a small sub-group who undergo FB with RED at a very young age. Unfortunately, none of these patients fulfilled the inclusion criteria. When considering patients younger than the age of three, factoring in maxillary patterns of growth and the phenotypic severity of those undergoing early significant interventions, it would be unwise to suggest our findings would be translatable for this age group.

The reliability of landmarks was consistent with previous three-dimensional landmarking studies. It is generally appreciated that certain validated landmarks on two-dimensional cephalometry are challenging to translate onto meshes as they represent singular points on curved surfaces. This limitation is easily offset by the additional insight gained through seeing points move through more than two axes[22-24]. A further difficulty when looking at FB is that points that have been purported as reliable for three-dimensional cephalometry, such as the nasopalatine foramen, are involved in the midline osteotomy and cannot be used[25]. Regardless, the landmarks in this study demonstrated excellent agreement on the whole.

Future

Planning, quantifying and evaluating craniofacial surgical movements in three dimensions is now the gold standard. Semi-automated workflows such as that described in this study will likely become automated in the future and provide us with the ability to fully understand and evaluate the management of rare conditions where there is such variability in surgical approaches internationally[26,27].

CONCLUSION

This study uses novel methodology to demonstrate that passive dental relapse occurs following facial bipartition whilst the surgical result remains stable. It may be appropriate to delay active orthodontic for six-months post-operatively until completion of this early compensatory phase.

CRediT Author Statement

AJR and LSvdL: Methodology, Validation, Data Curation, Writing – Original Draft. **EOS:** Methodology, Software, Validation, Formal Analysis, Data Curation, Writing – Review and Editing. **JO and RDE:** Conceptualisation, Resources, Writing – Review and Editing. **DSG:** Methodology, Conceptualisation, Resources, Writing – Review and Editing. **SS:** Supervision, Project Administration, Funding Acquisition, Writing – Review and Editing. **DD:** Methodology, Supervision, Project Administration, Funding Acquisition, Writing – Review and Editing.

Conflict of Interest

The authors have no conflicts of interest to declare nor do they have a financial interest in any of the products, devices, or drugs mentioned in this manuscript.

Funding

This work has been funded by Great Ormond Street Hospital for Children Charity (Grant No. 12SG15), the Engineering and Physical Sciences Research Council (EP/N02124X/1) and the European Research Council (ERC-2017-StG-757923). This report incorporates independent research from the National Institute for Health Research Biomedical Research Centre Funding Scheme. The views expressed in this publication are those of the authors and not necessarily those of the NHS, the National Institute for Health Research or the Department of Health. The funders had no role in study design, collection, analysis and interpretation of the data, decision to publish, or preparation of the manuscript.

REFERENCE LIST

1. Tessier P. Apert’s syndrome: Acrocephalosyndactyly type I. *Craniofacial Surgery Boston: Little, Brown.* 1985;280.
2. Apert E. De l’acrocéphalosyndactylie. *Bulletins et mémoires de la Société medicale des hôpitaux de Paris.* 1906;23:1310.
3. Firmin F, Coccaro PJ, Converse JM. Cephalometric analysis in diagnosis and treatment planning of craniofacial dysostoses. *Plast Reconstr Surg.* 1974;54(3):300-311.
4. Ortiz-Monasterio F, del Campo AF, Carrillo A. Advancement of the orbits and the midface in one piece, combined with frontal repositioning, for the correction of Crouzon's deformities. *Plast Reconstr Surg.* 1978;61(4):507-516.
5. Tessier P. The definitive plastic surgical treatment of the severe facial deformities of craniofacial dysostosis. Crouzon's and Apert's diseases. *Plast Reconstr Surg.* 1971;48(5):419-442.
6. van der Meulen JC. Medial faciotomy. *Br J Plast Surg.* 1979;32(4):339-342.
7. Tessier P. Facial Bipartition: A Concept More Than a Procedure. 1987; Berlin, Heidelberg.
8. McCarthy JG, Schreiber J, Karp N, Thorne CH, Grayson BH. Lengthening the human mandible by gradual distraction. *Plast Reconstr Surg.* 1992;89(1):1-8; discussion 9-10.
9. McCarthy JG, Stelnicki EJ, Mehrara BJ, Longaker MT. Distraction osteogenesis of the craniofacial skeleton. *Plast Reconstr Surg.* 2001;107(7):1812-1827.

10. Polley JW, Figueroa AA. Management of severe maxillary deficiency in childhood and adolescence through distraction osteogenesis with an external, adjustable, rigid distraction device. *J Craniofac Surg.* 1997;8(3):181-185; discussion 186.

11. Greig AV, Britto JA, Abela C, et al. Correcting the typical Apert face: combining bipartition with monobloc distraction. *Plast Reconstr Surg.* 2013;131(2):219e-230e.

12. Bell WH, Epker BN. Surgical-orthodontic expansion of the maxilla. *Am J Orthod.* 1976;70(5):517-528.

13. Koudstaal MJ, Wolvius EB, Schulten AJ, Hop WC, van der Wal KG. Stability, tipping and relapse of bone-borne versus tooth-borne surgically assisted rapid maxillary expansion; a prospective randomized patient trial. *Int J Oral Maxillofac Surg.* 2009;38(4):308-315.

14. Booth J, Roussos A, Ponniah A, Dunaway D, Zafeiriou S. Large scale 3D morphable models. *International Journal of Computer Vision.* 2018;126(2-4):233-254.

15. Posnick JC, Waitzman A, Armstrong D, Pron G. Monobloc and facial bipartition osteotomies: quantitative assessment of presenting deformity and surgical results based on computed tomography scans. *Journal of oral and maxillofacial surgery.* 1995;53(4):358-367.

16. Tessier P, Guiot G, Derome P. Orbital hypertelorism: II. Definite treatment of orbital hypertelorism (OR. H.) by craniofacial or by extracranial osteotomies. *Scandinavian journal of plastic and reconstructive surgery.* 1973;7(1):39-58.

17. Ponniah AJ, Witherow H, Richards R, Evans R, Hayward R, Dunaway D. Three-dimensional image analysis of facial skeletal changes after monobloc and bipartition distraction. *Plast Reconstr Surg.* 2008;122(1):225-231.

18. Gwanmesia I, Jeelani O, Hayward R, Dunaway D. Frontofacial advancement by distraction osteogenesis: a long-term review. *Plast Reconstr Surg.* 2015;135(2):553-560.
19. Raposo-Amaral CE, Denadai R, Zanco GL, Ghizoni E, Raposo-Amaral CA. Long-Term Follow-Up on Bone Stability and Complication Rate after Monobloc Advancement in Syndromic Craniosynostosis. *Plastic and Reconstructive Surgery.* 2020;145(4):1025-1034.
20. Proffit WR. Equilibrium theory revisited: factors influencing position of the teeth. *Angle Orthod.* 1978;48(3):175-186.
21. Raposo-Amaral CE, Denadai R, Ghizoni E, Raposo-Amaral CA. Treating craniofacial dysostoses with hypertelorism by monobloc facial bipartition distraction: Surgical and educational videos. *Plastic and reconstructive surgery.* 2019;144(2):433-438.
22. Gwilliam JR, Cunningham SJ, Hutton T. Reproducibility of soft tissue landmarks on three-dimensional facial scans. *Eur J Orthod.* 2006;28(5):408-415.
23. Hajeer MY, Ayoub AF, Millett DT, Bock M, Siebert JP. Three-dimensional imaging in orthognathic surgery: the clinical application of a new method. *Int J Adult Orthodon Orthognath Surg.* 2002;17(4):318-330.
24. Lagravere MO, Low C, Flores-Mir C, et al. Intraexaminer and interexaminer reliabilities of landmark identification on digitized lateral cephalograms and formatted 3-dimensional cone-beam computerized tomography images. *Am J Orthod Dentofacial Orthop.* 2010;137(5):598-604.
25. Han MD, Momin MR, Munaretto AM, Hao S. Three-dimensional cephalometric analysis of the maxilla: Analysis of new landmarks. *Am J Orthod Dentofacial Orthop.* 2019;156(3):337-344.

26. Knoops PGM, Papaioannou A, Borghi A, et al. A machine learning framework for automated diagnosis and computer-assisted planning in plastic and reconstructive surgery. *Sci Rep.* 2019;9(1):13597.

27. Shetye PR, Davidson EH, Sorkin M, Grayson BH, McCarthy JG. Evaluation of three surgical techniques for advancement of the midface in growing children with syndromic craniosynostosis. *Plast Reconstr Surg.* 2010;126(3):982-994.

LEGENDS

Figure 1.

Overlapping three-dimensional meshes following non-rigid iterative closest point registration demonstrating close alignment at the skull base and posterior cranial vault. This facilitates accurate measurement of the displacements of the frontofacial segment relative to these stable landmarks during later quantification.

Figure 2.

A diagram demonstrating the position of the manually placed landmarks used to improve conformance of non-rigid iterative closest point registration. 1 right zygomaticofrontal suture; 2 left zygomaticofrontal suture; 3 right supraorbital foramen; 4 left supraorbital foramen; 5 most antero-inferior point, right infraorbital rim; 6 most antero-inferior point, left infraorbital rim; 7 right infraorbital foramen; 8 left infraorbital foramen; 9 A Point 1 / Right A Point*; 10 A Point 2 / Left A Point; 11 mesial incisal tip of upper right central incisor; 12 mesial incisal tip of upper left central incisor; 13 right greater palatine foramen; 14 left greater palatine foramen; 15 mesiobuccal cusp tip or upper right first molar; 16 mesiobuccal cusp tip or upper left first molar; 17 midpoint of spheno-occipital synchondrosis; 18 right hamular process of pterygoid; 19 left hamular process of pterygoid; 20 basion; 21 opisthion; 22 most anterior point of right carotid canal; 23 most anterior point of left carotid canal.

* The A point was landmarked twice on the same location on the pre-operative mesh to allow for divergence of this point following sagittal osteotomy.

Figure 3.

Arrow maps for patients A, B and C show the displacements from an oblique and inferior view between the meshes from the pre-operative and the initial post-operative imaging on the left. On the right, the figure shows the displacements between the first, earlier post-operative mesh and the second, later mesh. For patients D and E, on the left, the pairs of images demonstrate the displacements between the pre-operative and initial post-operative movements. The middle pairs show the displacements between the initial post-operative and second post-operative meshes. Finally, the pairs, in the image on the right, show the displacements between the second and third sets of post-operative imaging.

Video 1.

Quantifying movements – demonstrated here in more detail are the arrow maps for patient A.

Supplemental Table 1.

Patient demographics.

Supplemental Table 2.

Reliability of Landmarks Between Observations

* The A point was landmarked twice on the same location on the pre-operative mesh to allow for divergence of this point following midline osteotomy.

Supplemental Table 3.

Point-to-point displacement of each landmark.

* The mean landmark co-ordinate between the first and second observations of each landmark were taken and the distance between the averages calculated.

Supplemental Table 4

Transverse (x-axis) Distances Between Paired Landmarks.

* The A point was landmarked twice on the same location on the pre-operative mesh to allow for divergence of this point following sagittal osteotomy.

Figure 1

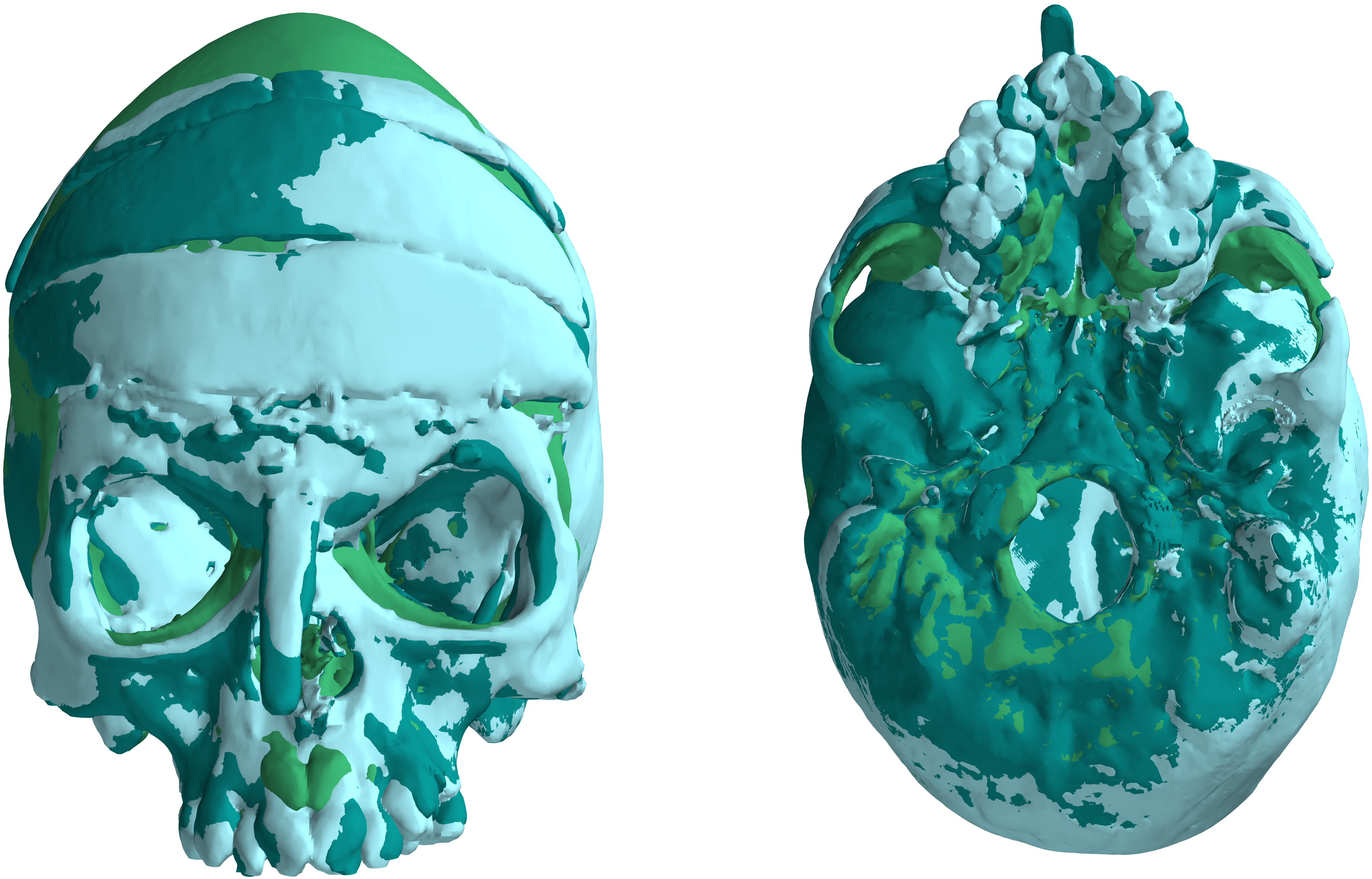

Figure 2

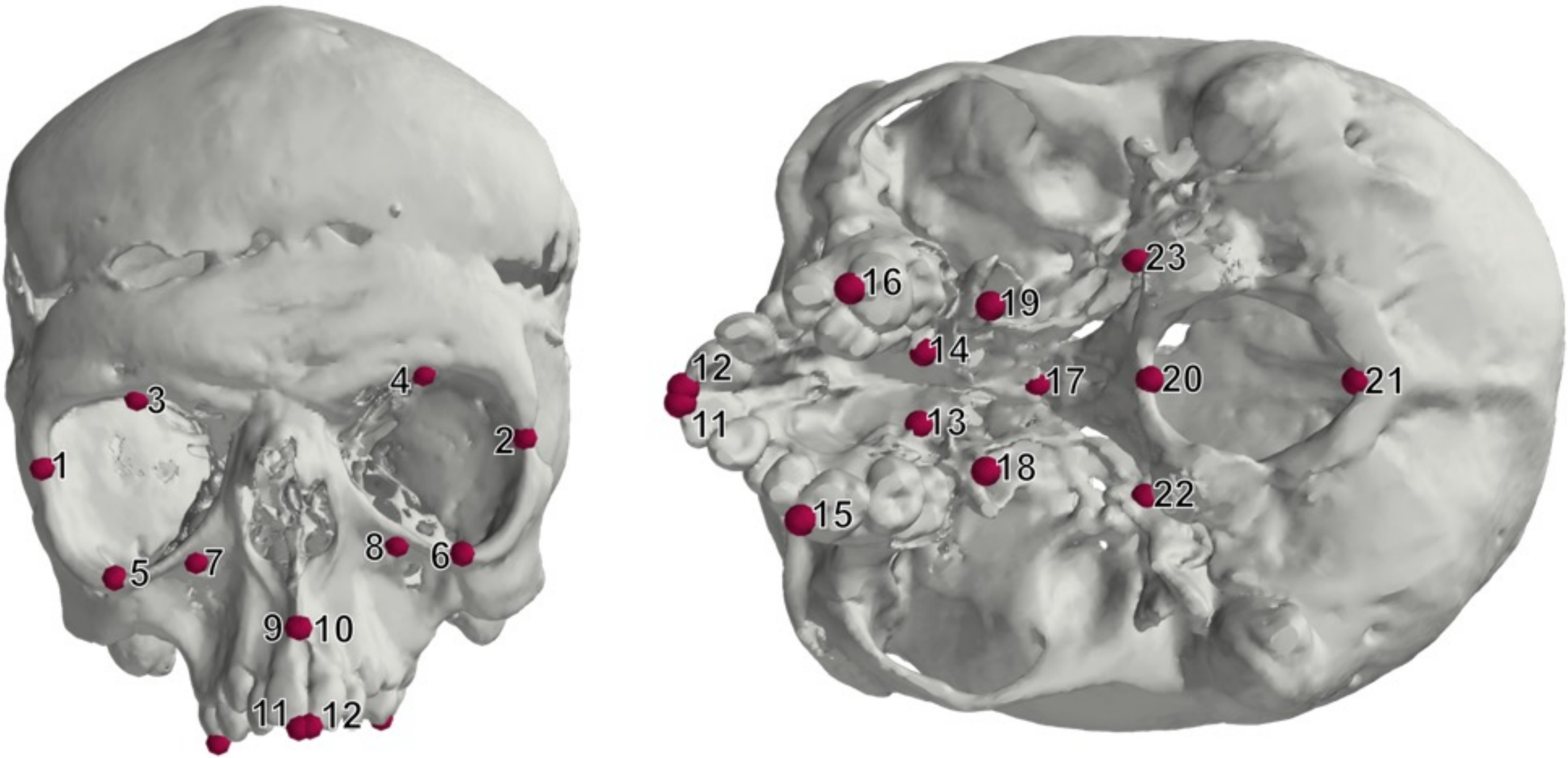

Figure 3

Video Still (to be used as thumbnail)

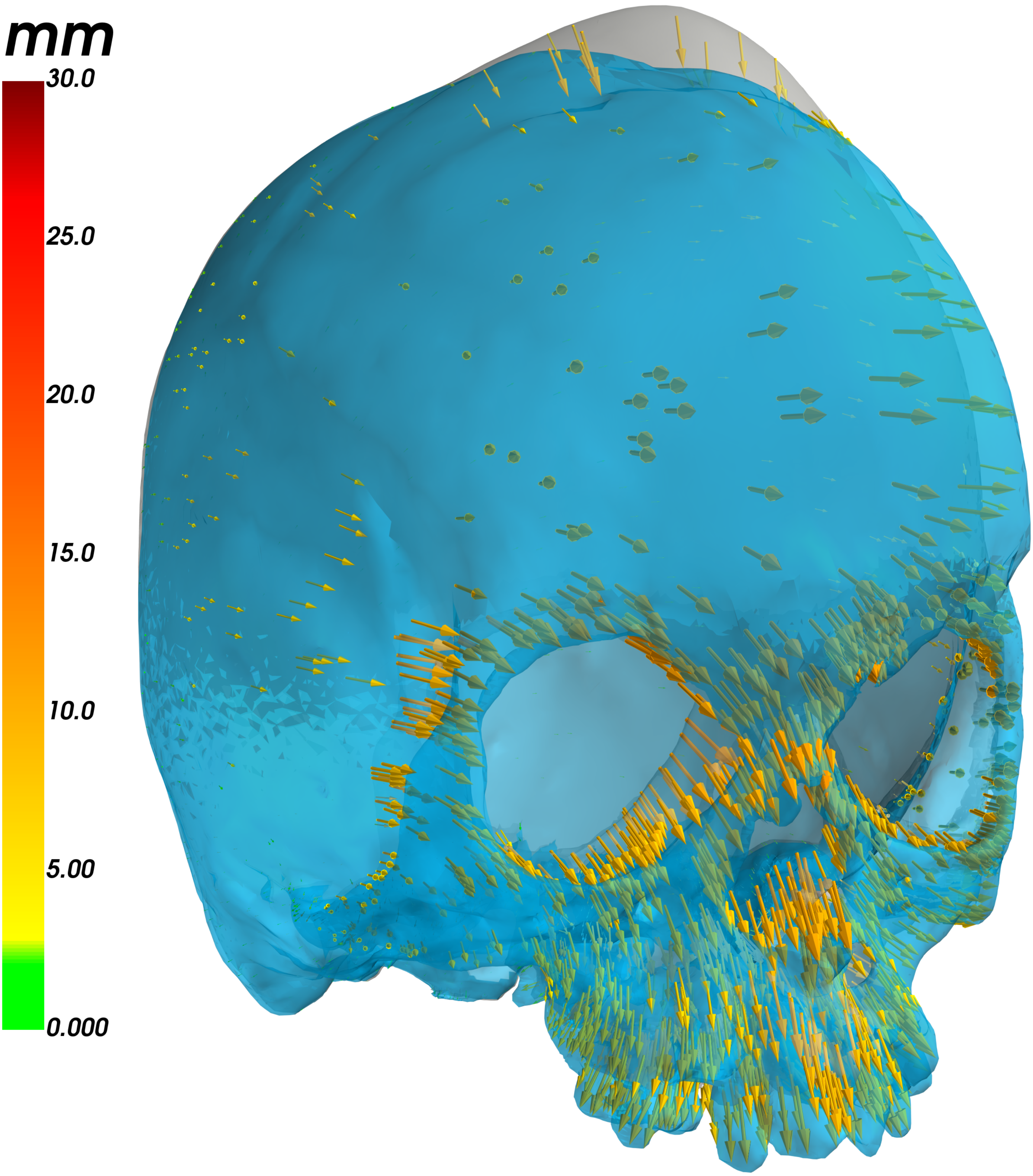

Supplemental Table 1 - Patient demographics

					Number of Days between each scan and time of operation			
Patient	**Diagnosis**	**Gender**	**Operation**	**Age at Operation**	**Pre-Op**	**Post-Op 1**	**Post-Op 2**	**Post-Op 3**
A	Apert	F	FB-RED	13	389	56	479	-
B	Apert	F	FB	21	76	32	164	-
C	Apert	M	FB-RED	6	6	63	387	-
D	Apert	M	FB-RED	18	566	57	198	387
E	Apert	F	FB-RED	13	57	63	244	553

Supplemental Table 2 - Reliability of Landmarks Between Observations

			Difference Between Landmarked Points at 1st and 2nd Observations (mm)																		
Patient			**A**			**B**			**C**			**D**				**E**					
																				Reliability	
Landmark			Pre-Op	1st Post Op Scan	2nd Post Op Scan	Pre-Op	1st Post Op Scan	2nd Post Op Scan	Pre-Op	1st Post Op Scan	2nd Post Op Scan	Pre-Op	1st Post Op Scan	2nd Post Op Scan	3rd Post Op Scan	Pre-Op	1st Post Op Scan	2nd Post Op Scan	3rd Post Op Scan	**Mean Distance Between Observations (mm)**	**Standard Deviation**
1	Zygomaticofrontal suture	R	0.75	1.82	1.15	0.66	0.57	1.31	0.49	0.33	0.71	1.89	1.61	0.94	0.83	0.72	0.37	0.34	0.37	0.78	0.45
2		L	0.36	0.44	0.43	0.93	0.80	1.41	0.48	0.07	1.31	0.61	1.61	1.13	2.17	0.61	0.48	0.55	0.48	0.87	0.52
3	Supraorbital foramen	R	0.88	1.13	2.51	0.38	1.15	2.48	3.07	2.46	0.82	0.87	0.58	1.67	0.61	1.25	0.49	1.15	0.25	1.21	0.80
4		L	1.24	2.72	0.75	1.41	0.43	0.13	2.08	1.20	0.89	0.34	0.97	1.73	1.30	0.43	0.98	0.80	1.40	0.99	0.51
5	Antero-inferior point, infraorbital rim	R	1.99	1.38	1.40	1.00	1.11	0.73	0.79	2.90	1.85	3.45	2.11	1.24	1.24	1.59	1.58	1.26	2.53	1.61	0.77
6		L	2.04	0.77	0.35	2.67	0.14	0.94	0.19	1.81	1.14	1.56	0.97	0.27	2.83	0.93	1.39	2.05	0.76	1.23	0.78
7	Infraorbital foramen	R	0.49	0.34	0.44	1.37	0.51	0.27	0.34	0.41	0.81	0.40	0.35	0.19	0.07	0.22	0.67	0.76	0.98	0.51	0.33
8		L	0.80	0.44	0.89	1.90	0.97	0.27	0.05	0.54	0.41	0.53	0.67	0.22	0.71	0.26	0.73	0.47	0.49	0.58	0.41
9	A Point*	R	1.56	0.81	1.90	0.41	1.01	1.05	0.55	0.36	2.19	0.54	0.12	0.52	0.63	0.38	0.44	1.26	2.63	0.86	0.66
10		L	1.51	0.43	2.88	0.42	1.16	1.32	0.64	2.61	1.13	0.50	0.19	0.66	1.47	0.41	0.22	2.05	3.27	1.14	0.84
11	Mesial incisal tip of upper central incisor	R	0.42	0.34	0.98	0.51	0.69	0.17	0.20	0.60	0.28	0.50	0.21	0.55	0.28	0.75	0.19	0.34	0.17	0.38	0.19
12		L	0.31	1.08	0.38	0.45	0.60	0.49	0.37	0.15	0.80	0.61	0.32	0.69	0.28	0.68	0.14	0.40	0.56	0.45	0.19
13	Greater palatine foramen	R	2.25	2.12	3.21	1.10	1.03	0.87	1.91	2.18	1.10	0.90	1.53	3.45	0.18	0.01	2.83	2.49	1.31	1.47	0.89
14		L	1.63	1.63	2.95	0.80	1.69	0.34	1.66	0.67	0.35	1.32	0.50	3.22	0.99	0.73	0.16	0.72	1.02	1.01	0.71
15	Mesiobuccal cusp tip or upper first molar	R	2.09	1.29	0.46	0.43	1.03	2.81	0.55	1.05	1.01	0.83	0.55	0.83	1.74	0.59	1.00	1.38	0.68	1.01	0.57
16		L	1.16	1.74	0.45	2.43	1.59	0.85	0.19	0.67	0.13	0.61	1.03	0.20	1.73	0.91	1.67	0.30	0.14	0.88	0.65
17	Midpoint of spheno-occipital synchondrosis		1.48	1.66	1.10	0.87	0.98	0.76	0.23	0.08	2.53	0.23	0.90	0.55	0.17	0.34	1.28	1.93	1.42	0.87	0.65
18	Hamular process of pterygoid	R	0.21	0.23	0.22	0.58	0.16	0.07	0.49	0.11	0.10	0.04	0.21	0.30	0.54	0.49	0.30	0.05	0.23	0.26	0.18
19		L	0.47	0.29	0.28	0.37	0.29	0.25	0.39	0.39	0.22	0.25	0.13	0.68	0.40	0.13	0.37	0.52	0.16	0.31	0.15
20	Basion		1.15	0.90	0.89	0.65	0.85	0.48	0.51	0.71	0.77	0.52	0.41	1.24	0.24	0.54	0.37	0.60	1.23	0.63	0.28
21	Opisthion		0.55	0.26	0.06	0.76	0.52	0.72	1.72	0.75	0.72	0.92	0.19	0.37	0.72	0.08	0.15	1.01	0.75	0.65	0.38
22	Most anterior point of carotid canal	R	1.08	0.56	0.41	0.62	0.43	0.35	0.59	1.08	1.00	0.44	0.95	0.74	0.36	0.25	0.76	0.50	0.83	0.61	0.25
23		L	0.99	0.43	0.72	0.35	0.33	1.05	0.20	0.46	0.35	1.25	0.38	0.37	0.24	0.63	0.61	1.07	1.15	0.59	0.34

* The A point was landmarked twice on the same location on the pre-operative mesh to allow for divergence of this point following midline osteotomy.

Supplemental Table 3 - Point-to-point displacement of each landmark

			Mean Displacements Between Landmarks (mm)*											
			Patient A		Patient B		Patient C		Patient D			Patient E		
	Landmark		Pre to Post Op 1	Post Op 1 to Post Op 2	Pre to Post Op 1	Post Op 1 to Post Op 2	Pre to Post Op 1	Post Op 1 to Post Op 2	Pre to Post Op 1	Post Op 1 to Post Op 2	Post Op 2 to Post Op 3	Pre to Post Op 1	Post Op 1 to Post Op 2	Post Op 2 to Post Op 3
1	Zygomaticofrontal suture	R	10.4	1.8	6.0	1.5	12.6	1.2	15.9	2.2	3.3	14.8	1.8	1.3
2		L	11.5	1.2	6.5	2.2	8.6	4.4	10.3	4.6	3.4	9.2	0.7	1.1
3	Supraorbital foramen	R	14.3	2.3	8.9	0.9	12.4	3.2	18.2	1.7	4.2	10.5	1.4	1.3
4		L	15.0	1.7	5.7	1.4	7.5	4.6	14.5	9.6	2.4	10.1	1.7	0.8
5	Antero-inferior point, infraorbital rim	R	8.4	3.7	7.3	1.2	11.3	2.2	15.2	1.6	0.7	10.5	1.2	0.8
6		L	9.9	1.6	7.7	1.1	11.1	4.9	9.5	1.2	1.7	9.1	2.2	0.8
7	Infraorbital foramen	R	8.5	1.6	7.9	1.3	14.2	1.6	13.1	2.4	2.4	9.8	1.2	0.9
8		L	9.0	1.0	7.6	1.4	13.0	1.4	11.3	2.9	2.8	9.8	1.1	0.9
9	A Point	R	11.1	1.0	6.3	1.8	14.0	3.6	10.3	2.6	2.5	8.2	2.5	0.7
10		L	11.0	1.1	6.1	2.0	13.6	1.4	10.2	2.6	2.2	8.1	2.5	1.1
11	Mesial incisal tip of upper central incisor	R	9.3	1.8	5.9	0.9	10.6	2.6	9.6	3.8	2.6	9.4	0.3	1.1
12		L	10.0	1.8	7.9	1.1	11.7	4.4	10.3	1.2	1.7	10.0	1.7	1.2
13	Greater palatine foramen	R	10.7	1.8	7.0	0.9	13.7	2.3	14.7	3.4	3.2	8.6	1.8	2.4
14		L	8.5	0.8	8.6	1.5	13.2	1.9	13.1	2.4	3.2	9.4	1.6	1.6
15	Mesiobuccal cusp tip or upper first molar	R	7.7	1.3	9.4	2.1	11.4	2.3	12.7	3.2	1.6	8.7	0.6	1.2
16		L	7.4	1.0	14.4	4.5	13.5	4.1	11.8	2.4	3.3	10.1	1.4	2.0
17	Midpoint of spheno-occipital synchondrosis		1.4	1.0	0.9	0.6	1.0	2.9	1.0	1.6	1.5	0.9	0.8	0.9
18	Hamular process of pterygoid	R	1.6	1.4	5.8	1.1	3.4	3.7	2.7	1.9	2.1	2.9	0.7	1.4
19		L	1.7	0.8	3.0	0.3	2.8	2.7	2.8	2.0	1.6	2.0	1.2	0.7
20	Basion		1.2	1.0	0.3	0.4	1.7	1.2	1.5	0.5	0.7	0.8	0.7	0.5
21	Opisthion		0.8	0.1	0.6	1.0	2.2	1.2	0.9	0.7	1.2	0.8	0.8	1.0
22	Most anterior point of carotid canal	R	0.5	0.8	1.1	1.1	1.1	1.1	1.9	2.2	0.3	1.1	0.8	0.6
23		L	0.6	0.5	0.5	0.9	1.8	1.0	1.6	1.8	1.1	0.9	1.0	0.8

* The mean landmark co-ordinate between the first and second observations of each landmark were taken and the distance between the averages calculated.

Supplemental Table 4 - Transverse (x-axis) Distances Between Paired Landmarks

		Changes in Transverse Distances Between Paired Landmarks (mm)											
		Patient A		Patient B		Patient C		Patient D			Patient E		
	Paired Left and Right Landmarks	Pre to Post Op 1	Post Op 1 to Post Op 2	Pre to Post Op 1	Post Op 1 to Post Op 2	Pre to Post Op 1	Post Op 1 to Post Op 2	Pre to Post Op 1	Post Op 1 to Post Op 2	Post Op 2 to Post Op 3	Pre to Post Op 1	Post Op 1 to Post Op 2	Post Op 2 to Post Op 3
1 **2**	Zygomaticofrontal sutures	-8.0	1.2	-4.4	0.0	-2.9	4.1	-6.3	1.3	0.9	-4.8	-0.5	-0.9
3 **4**	Supraorbital foramina	-12.1	1.1	-12.6	2.4	-2.3	4.5	-12.3	8.6	1.0	-8.6	0.5	0.2
5 **6**	Antero-inferior points, infraorbital rim	-5.2	-3.2	-1.9	-2.2	-0.8	4.5	-6.9	-0.6	1.6	-0.2	-0.9	-0.7
7 **8**	Infraorbital foramina	-1.5	-0.7	-2.8	0.6	3.4	-0.1	-1.3	0.6	-0.3	-2.2	1.4	1.3
9 **10**	A Point*	2.8	-1.2	0.1	0.0	4.6	-3.7	1.6	0.0	-0.1	1.4	0.8	0.1
11 **12**	Mesial incisal tip of upper central incisors	1.3	0.5	-2.4	0.1	2.1	2.3	1.8	-2.8	0.9	0.8	-1.3	-0.3
13 **14**	Greater palatine foramina	6.2	-0.9	2.8	-0.2	3.1	-0.1	7.9	-4.2	0.5	2.5	0.5	-1.0
15 **16**	Mesiobuccal cusp tip or upper first molars	8.4	0.4	0.7	0.4	10.0	-3.6	7.9	-1.8	-1.8	7.9	-1.8	-1.4

* The A point was landmarked twice on the same location on the pre-operative mesh to allow for divergence of this point following sagittal osteotomy.